

# LLM-Free Image Captioning Evaluation in Reference-Flexible Settings

Shinnosuke Hirano, Yuiga Wada, Kazuki Matsuda, Seitaro Otsuki, Komei Sugiura

Keio University

{shinhirano, yuiga, k2matsuda0, otsu8sei14, komei.sugiura}@keio.jp

## Abstract

We focus on the automatic evaluation of image captions in both reference-based and reference-free settings. Existing metrics based on large language models (LLMs) favor their own generations; therefore, the neutrality is in question. Most LLM-free metrics do not suffer from such an issue, whereas they do not always demonstrate high performance. To address these issues, we propose Pearl, an LLM-free supervised metric for image captioning, which is applicable to both reference-based and reference-free settings. We introduce a novel mechanism that learns the representations of image-caption and caption-caption similarities. Furthermore, we construct a human-annotated dataset for image captioning metrics, that comprises approximately 333k human judgments collected from 2,360 annotators across over 75k images. Pearl outperformed other existing LLM-free metrics on the Composite, Flickr8K-Expert, Flickr8K-CF, Nebula, and FOIL datasets in both reference-based and reference-free settings. Our project page is available at <https://pearl.kinsta.page/>.

## Introduction

Image captioning has been widely studied and utilized in various applications, including assisting visually impaired people and providing explanations in robotics. The efficient development of image captioning models relies on automatic evaluation metrics that closely align with human judgments. Recent efforts have focused on building metrics that correlate more strongly with human evaluations than classic metrics such as CIDEr (Vedantam, Zitnick, and Parikh 2015). Although this task has been widely investigated, it remains challenging even for state-of-the-art (SOTA) metrics (e.g. Yao et al. (2024); Kim et al. (2025)). Indeed, the correlations of these metrics with human judgments are still lower than the correlations among human judgments (Lee et al. 2024; Hodosh et al. 2013). Therefore, constructing aligned metrics would be beneficial for both the image captioning community and society.

Previous studies have shown that existing metrics based on LLMs favor their own generations (Panickssery, Bowman, and Feng 2024; Navigli, Conia, and Ross 2023). Moreover, they often suffer from prohibitively long inference times, which makes their application impractical. Therefore, it is important to develop an LLM-free metric that does not suffer from the neutrality and speed issues.

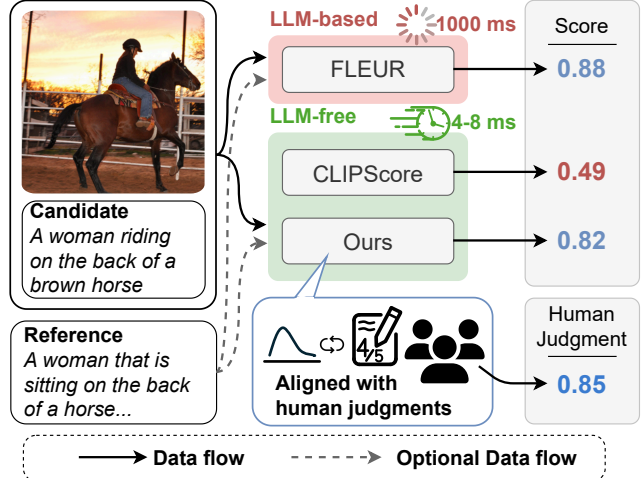


Figure 1: Pearl is an LLM-free automatic evaluation metric for image captioning. Pearl works significantly faster than slow LLM-based metrics; thus it is suitable for fast development cycles of practical image captioning models. Moreover, Pearl is the first LLM-free supervised metric that can handle both reference-based and reference-free evaluation with a single supervised model.

LLM-free metrics (Sarto, Barraco et al. 2023; Matsuda et al. 2024; Sarto, Moratelli et al. 2024) are significantly faster than LLM-based metrics. However, they exhibit several notable issues. For example, although supporting both reference-based and reference-free evaluation is important for practical applications (Tong, He et al. 2024), few demonstrate high performance in both settings. This is partially because metrics that support both settings (Hessel, Holtzman et al. 2021; Sarto, Moratelli et al. 2024) simply compute cosine similarity between embeddings from encoders such as CLIP (Radford et al. 2021), which can be less aligned with human judgments (Wada et al. 2024). Moreover, supervised metrics employ fixed representations for similarity (e.g. RUSE (Shimanaka et al. 2018)), which may be suboptimal because of the lack of representation learning.

To address these issues, we propose Pearl, a supervised automatic evaluation metric for image captioning. Fig. 1 shows an overview of Pearl. In addition to its LLM-free

nature, Pearl differs from existing approaches in several respects. First, unlike other learning-based metrics (Lee, Yoon et al. 2021; Wada et al. 2024), Pearl is a single model capable of evaluating captions in both reference-based and reference-free settings. Second, we introduce the Adaptive RUSe-type Similarity Mechanism to learn the representations of image–caption and caption–caption similarities.

To train Pearl, we construct a new dataset, Spica, which includes 333K human judgments for a diverse collection of image–caption pairs. The Spica dataset stands out with its significantly larger number of human judgments and greater diversity of both images and annotators compared with other standard datasets (Aditya et al. 2015; Hodosh et al. 2013; Lee, Yoon et al. 2021; Wada et al. 2024; Matsuda et al. 2024). Specifically, it includes approximately 333K human judgments, which is 2.5 times the number of human judgments in the dataset previously recognized as having the largest number of human judgments.

Our key contributions are as follows:

- We introduce the Image-Guided Evaluation Module and the Reference-Guided Evaluation Module to handle the similarities, which enables both reference-based and reference-free evaluation with a single model.
- We constructed Spica, a publicly available dataset for image captioning metrics, which is significantly larger than previous datasets. Specifically, it contains 75,535 images and 333,397 human judgments from 2,360 annotators.
- We achieved SOTA performance on standard benchmarks within LLM-free metrics, enabling practical large-scale candidate caption evaluation.

## Related Work

### LLM-free Metrics

**Reference-based metrics.** Standard reference-based metrics include BLEU (Papineni et al. 2002), METEOR (Banerjee et al. 2005), ROUGE (Lin 2004), CIDEr (Vedantam, Zitnick, and Parikh 2015), and SPICE (Anderson et al. 2016; Wada, Kaneda, and Sugiura 2023), which evaluate captions using rule-based approaches based only on reference captions.

In contrast, several reference-based metrics also incorporate images. Notable metrics include ViLBERTScore (Lee et al. 2020), which feeds image–caption and caption–caption pairs into ViLBERT (Lu et al. 2019) and calculates the cosine similarities. Recent metrics (Wada et al. 2024; Matsuda et al. 2024) adopt a supervised approach, directly learning to evaluate captions from human judgments. These metrics are based on the RUSe-type similarity (Shimanaka et al. 2018; Rei et al. 2020), which merely computes fixed representations of the element-wise difference and Hadamard product.

**Reference-free metrics.** Reference-free metrics such as CLIPScore (Hessel, Holtzman et al. 2021) rely only on images for evaluating candidate captions. CLIPScore calculates scores by computing the cosine similarity between the embeddings of CLIP (Radford et al. 2021). Sarto et al. (Sarto, Barraco et al. 2023) highlighted that CLIP was

trained on alt-texts, whose text distribution significantly differs from that of image captions; they therefore proposed PAC-S and PAC-S++ (Sarto, Moratelli et al. 2024), variants of CLIPScore, which employ CLIP finetuned by generated images and captions. BLIP2Score (Zeng et al. 2024b) evaluates candidate captions in a manner similar to that of CLIP-Score by using embeddings of BLIP-2 (Li et al. 2023).

### LLM-based Metrics

LLM-based metrics use LLM or MLLM in its evaluation process. Various studies (Chan, Petryk et al. 2023; Lee et al. 2024; Ohi et al. 2024; Tong, He et al. 2024; Yao et al. 2024; Zeng et al. 2024a; Kim et al. 2025; Matsuda et al. 2025) have proposed LLM/MLLM-based metrics for image captioning. CLAIR (Chan, Petryk et al. 2023) is the first metric that leverages LLMs in a zero-shot manner to compare references and candidate captions. While CLAIR evaluates the captions without considering images, FLEUR (Lee et al. 2024) utilizes LLaVA (Liu, Li et al. 2023; Liu et al. 2024) to incorporate images. FLEUR introduces score smoothing, which calibrates the raw score by the probabilities associated with output tokens. Similarly, EXPERT (Kim et al. 2025) first produces the evaluation score using score smoothing, and then generates a brief explanation based on three criteria — *fluency*, *relevance*, and *descriptiveness*. On the other hand, HiFi-Score (Yao et al. 2024) converts captions and images into hierarchical parsing graphs by LLMs, and compares them through fine-grained graph matching.

## Methodology

We propose Pearl, an LLM-free supervised automatic evaluation metric for image captioning, which is applicable to both reference-based and reference-free settings. Pearl adopts a single-model strategy that jointly addresses both settings, facilitating the learning of shared representations. In contrast to approaches that train separate models for each setting, this design allows all samples – whether reference-based or reference-free – to contribute to training.

The inputs to Pearl are an image  $x_{\text{img}}$ , a candidate caption  $x_{\text{cand}}$ , and a set of references  $X_{\text{ref}}$ . In the reference-based setting,  $X_{\text{ref}} = \{x_{\text{ref}}^{(i)}\}_{i=1}^N$ , where  $N \geq 1$  and each reference  $x_{\text{ref}}^{(i)}$  is represented as a binary matrix  $x_{\text{ref}}^{(i)} \in \{0, 1\}^{V \times L}$ . In the reference-free setting,  $X_{\text{ref}} = \emptyset$ , corresponding to  $N = 0$ . Here,  $V$  and  $L$  represent the vocabulary size and the number of tokens in a caption, respectively. In both settings,  $x_{\text{img}} \in \mathbb{R}^{3 \times H \times W}$  represents the input image, where  $H$  and  $W$  denote the height and width of the image, respectively. The candidate caption  $x_{\text{cand}} \in \{0, 1\}^{V \times L}$  is also encoded as a binary matrix. Given these inputs, Pearl outputs the final evaluation score  $\hat{y}$  in an LLM-free manner, with or without reference captions.

**Why do we need LLM-free metrics?** LLM-based metrics have two severe limitations. First, recent studies have shown that LLM-based evaluators favor their own generations (Panickssery, Bowman, and Feng 2024; Navigli, Cohn, and Ross 2023); therefore, their neutrality is in question. Second, as will be discussed in the *Experiments* section,

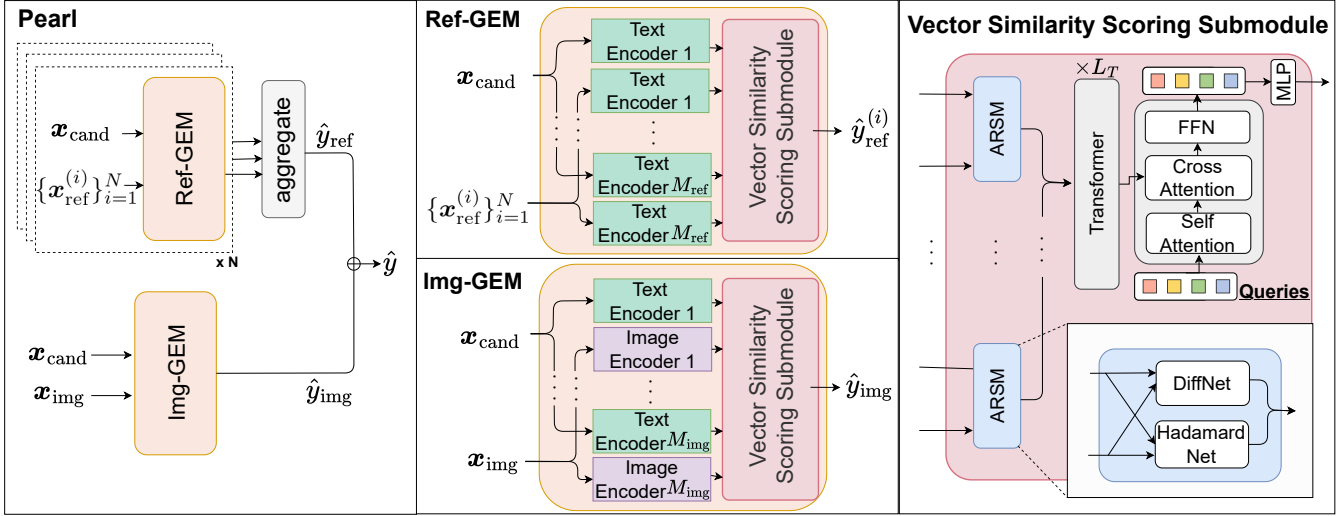


Figure 2: Overview of the proposed metric, Pearl. Our proposed metric consists of the Img-GEM and multiple Ref-GEMs. The Img-GEM computes a score for a candidate caption based on the associated image, whereas each Ref-GEM calculates a score based on a reference. In reference-based setting, Pearl computes the scores for candidate caption based on either the image or the references, and then fuses them into the final prediction score. Conversely, in the reference-free setting, the final prediction score is computed based solely on the image.

LLM-based metrics often suffer from prohibitively long inference times, making their application impractical. Therefore, it is important to develop an LLM-free metric that does not suffer from the neutrality and speed issues.

## Architecture Overview

Pearl consists of four main features: Adaptive RUSE-type Similarity Mechanism (ARSM), Image-Guided Evaluation module (Img-GEM), Reference-Guided Evaluation module (Ref-GEM), and Vector Similarity Scoring (VSS) submodule. Fig. 2 shows an overview of Pearl.

The core components of our proposed method are ARSM and VSS. ARSM can handle learnable representations of image–caption and caption–caption similarities, unlike previous metrics which rely on fixed representations (Rei et al. 2020; Shimanaka et al. 2018; Wada et al. 2024; Matsuda et al. 2024). ARSM can be applicable to existing supervised metrics for natural language generation (Shimanaka et al. 2018; Rei et al. 2020). In contrast, VSS generates an intermediate score for candidates from multiple perspectives by fusing embeddings from multiple encoders (e.g., CLIP, BLIP-2, BEiT-3). Specifically, it computes ARSM-based representations for each encoder independently and then fuses them to produce an intermediate score.

Building on these cores, the proposed metric consists of Img-GEM and  $N$  Ref-GEMs, each of which internally invokes VSS, where  $N$  denotes the number of references. First, Img-GEM evaluates candidate captions based on images using VSS, while each Ref-GEM assesses them based on reference captions, also using VSS. Subsequently, Pearl generates the final score by combining the  $N$  Ref-GEM outputs with the Img-GEM outputs. Unlike previous supervised metrics (Wada et al. 2024; Matsuda et al. 2024) that per-

form early fusion of features, we adopt a late-fusion approach, allowing effective learning in both reference-based and reference-free settings.

## Adaptive RUSE-type Similarity Mechanism

We introduce Adaptive RUSE-type Similarity Mechanism (ARSM), which learns representations of image–caption and caption–caption similarities. Previous approaches (e.g. Shimanaka et al. (2018)) often have utilized element wise differences and the Hadamard product as fixed representations for the similarity. This RUSE-type similarity operation has demonstrated its effectiveness in various tasks, including machine translation (Shimanaka et al. 2018; Rei et al. 2020) and image captioning (Wada et al. 2024; Matsuda et al. 2024). However, such fixed operations may be sub-optimal because they do not involve representation learning.

Although replacing the Hadamard product and element wise difference with feed-forward networks sounds theoretically plausible, this does not always yield effective results (see ablation studies in the *Experiments* section). Therefore, we construct feed-forward networks that satisfy the same input and output requirements as the Hadamard product and element wise difference. We then integrate this network in a trainable form into our proposed metric. We introduce two components of ARSM: DiffNet and HadamardNet.

**DiffNet.** DiffNet consists of a single layer of feed-forward networks. DiffNet replaces the difference operation between two features,  $x_1 \in \mathbb{R}^{n \times d}$  and  $x_2 \in \mathbb{R}^{n \times d}$ . The difference operation is easily captured by a single fully-connected layer with the following initialization parameters:  $o_{\text{diff}} = \mathbf{W}_1 x_1 + \mathbf{W}_2 x_2 + \mathbf{b}$ , where  $o_{\text{diff}}$  denotes the output of DiffNet,  $\mathbf{W}_1$  and  $\mathbf{W}_2$  are weight parameters, and  $\mathbf{b}$  is a bias

parameter. We initialize  $\mathbf{W}_1 = \mathbf{1}_{d \times n}$ ,  $\mathbf{W}_2 = -\mathbf{1}_{d \times n}$ , and  $\mathbf{b} = \mathbf{0}$ , where  $\mathbf{1}_{d \times n}$  denotes  $d \times n$  matrix of ones.

**HadamardNet.** HadamardNet, composed of  $L_h$  CNN layers, is used to capture the relationship between  $\mathbf{x}_1$  and  $\mathbf{x}_2$  instead of the Hadamard product operations. Given the challenges in constructing mappings of the Hadamard products using methods akin to DiffNet, we employ a learning-based approach. Initially, we generate multiple vectors from a uniform distribution  $U(a, b)$  to collect training samples. We then pretrain HadamardNet to learn the Hadamard products of these vectors. Here,  $a$  and  $b$  denotes the hyperparameters. We initialize HadamardNet with the parameters obtained from this pretraining. The final output of HadamardNet is  $\mathbf{o}_{\text{had}, L_h}$ . Finally, the output of ARSM is defined as  $\mathbf{o}_{\text{ARSM}} = [\mathbf{o}_{\text{diff}, L_d}; \mathbf{o}_{\text{had}, L_h}]$ .

## Img-GEM and Ref-GEM

Img-GEM and Ref-GEM handle image–caption and caption–caption similarities, respectively. Previous studies (Hessel, Holtzman et al. 2021; Sarto, Barraco et al. 2023; Lee et al. 2024) have noted that preparing high-quality references is extremely time-consuming and have proposed metrics for both settings (Lee et al. 2024; Sarto, Barraco et al. 2023). Although supervised metrics outperform other LLM-free metrics on standard benchmarks, almost all existing supervised metrics (Wada et al. 2024; Matsuda et al. 2024) assume a reference-based setting. This limitation arises because these metrics fuse the features of a candidate caption, references, and an image early in the process. In contrast, our supervised metric employs a late-fusion approach, computing scores from Img-GEM and multiple Ref-GEMs and then fusing these into the final prediction score.

Img-GEM computes a score for a candidate caption based on the associated image, while each Ref-GEM calculates a score based on a reference. Initially, in Img-GEM, we extract image features  $\{ \mathbf{v}_{\text{vgem}, j} \in \mathbb{R}^{d_{\text{vgem}, j}} \mid j = 1, 2, \dots, M_{\text{img}} \}$  from  $\mathbf{x}_{\text{img}}$  using  $M_{\text{img}}$  image encoders. Here,  $d_{\text{vgem}, j}$  denotes the dimension of the  $j$ -th encoder in Img-GEM. Subsequently, we also extract sentence embeddings  $\{ \mathbf{c}_{\text{vgem}, j} \in \mathbb{R}^{d_{\text{vgem}, j}} \mid j = 1, 2, \dots, M_{\text{img}} \}$  from  $\mathbf{x}_{\text{cand}}$  using the corresponding  $M_{\text{img}}$  text encoders. We use frozen CLIP (Radford et al. 2021), BLIP-2 (Li et al. 2023), and BEiT-3 (Wang et al. 2023) as the image and text encoders in Img-GEM because they are known for their ability to align image and text features.

The  $i$ -th Ref-GEM processes the  $i$ -th reference  $\mathbf{x}_{\text{ref}}^{(i)}$  and extracts sentence embeddings  $\{ \mathbf{r}_{\text{rgem}, j}^{(i)} \in \mathbb{R}^{d_{\text{rgem}, j}} \mid j = 1, 2, \dots, M_{\text{ref}} \}$  using  $M_{\text{ref}}$  text encoders. Here,  $d_{\text{rgem}, j}$  denotes the dimension of the  $j$ -th encoder in Ref-GEM. Similarly, we extract sentence embeddings  $\{ \mathbf{c}_{\text{rgem}, j} \in \mathbb{R}^{d_{\text{rgem}, j}} \mid j = 1, 2, \dots, M_{\text{ref}} \}$  from  $\mathbf{x}_{\text{cand}}$  using  $M_{\text{ref}}$  text encoders. As the text encoders in Ref-GEM, we use frozen BLIP-2, BEiT-3, and Stella (Zhang et al. 2024), a lightweight sentence embedding model with approximately 400M parameters. Here, Stella is employed because its performance is comparable to that of SOTA LLMs on standard benchmarks (e.g. Zhang et al. (2024)).

Subsequently, in Img-GEM, we feed the extracted  $\{ (\mathbf{c}_{\text{vgem}, j}, \mathbf{v}_{\text{vgem}, j}) \mid j = 1, 2, \dots, M_{\text{img}} \}$  into the VSS submodule. Moreover, Ref-GEM feeds the extracted  $\{ (\mathbf{c}_{\text{rgem}, j}, \mathbf{r}_{\text{rgem}, j}^{(i)}) \mid j = 1, 2, \dots, M_{\text{img}} \}$  into the same submodule. Finally, the Img-GEM output and the  $i$ -th Ref-GEM output are  $\mathbf{h}_{\text{img}}$  and  $\mathbf{h}_{\text{ref}}^{(i)}$ , respectively.

## Vector Similarity Scoring Submodule

VSS submodule evaluates  $\mathbf{x}_{\text{cand}}$  based on the inputs  $\{ (\mathbf{c}_i, \mathbf{h}_i) \mid i = 1, \dots, M \}$ , where  $\mathbf{c}_i$  and  $\mathbf{h}_i$  denote the  $i$ -th embedding of  $\mathbf{x}_{\text{cand}}$ , and the  $i$ -th embedding used as a basis for evaluating  $\mathbf{x}_{\text{cand}}$ , respectively. Here,  $M$  denotes the number of encoders. By fusing embeddings obtained from multiple encoders, VSS can assess  $\mathbf{x}_{\text{cand}}$  from multiple perspectives. Initially, this submodule employs ARSM on each pair  $(\mathbf{c}_i, \mathbf{h}_i)$  to obtain features  $\mathbf{g}_i$  that capture representations of differences between embeddings.

These features  $\{ \mathbf{g}_i \}_{i=1}^M$  are then concatenated and fed into a Transformer consisting of  $L_T$  layers to extract features  $\mathbf{g}_{\text{enc}}$  that are beneficial for evaluation. Inspired by (Li et al. 2023), we then feed  $\mathbf{g}_{\text{enc}}$  into a Q-Former, which contains  $L_Q$  layers, to obtain the feature  $\mathbf{g}_{\text{dec}}$ . Finally, the score  $\hat{y}_{\text{vc}}$  is obtained by processing  $\mathbf{g}_{\text{dec}}$  through an MLP.

In the reference-based setting, we compute the scores for  $\mathbf{x}_{\text{cand}}$  based on either  $\mathbf{x}_{\text{img}}$  or  $\{ \mathbf{x}_{\text{ref}}^{(i)} \}_{i=1}^N$  and then fuse them into the final prediction score. In the reference-free setting, the final prediction score for  $\mathbf{x}_{\text{cand}}$  is computed based solely on the image. The image-based score for  $\hat{y}_{\text{img}}$  and the reference-based score  $\hat{y}_{\text{ref}}$  are computed as follows:

$$\hat{y}_{\text{img}} = \sigma(\text{MLP}(\mathbf{h}_{\text{img}})), \quad (1)$$

$$\hat{y}_{\text{ref}} = \max_i \left( \sigma(\text{MLP}(\mathbf{h}_{\text{ref}}^{(i)})) \right), \quad (2)$$

where  $\sigma$  denotes the sigmoid function.

Finally, the final evaluation score  $\hat{y}$  is computed by fusing  $\hat{y}_{\text{img}}$  and  $\hat{y}_{\text{ref}}$  as follows:

$$\hat{y} = \begin{cases} \lambda \hat{y}_{\text{img}} + (1 - \lambda) \hat{y}_{\text{ref}} & \text{(Reference-based)} \\ \hat{y}_{\text{img}} & \text{(Reference-free)} \end{cases}, \quad (3)$$

where  $\lambda$  is a hyperparameter within  $[0, 1]$ . We set  $\lambda$  to 0.5. We use the Huber loss  $\mathcal{L}_{\text{huber}}(\cdot, \cdot)$  for its robustness to outliers. In the reference-based setting, the loss is computed as the average of  $\mathcal{L}_{\text{huber}}(y, \hat{y}_{\text{img}})$  and  $\mathcal{L}_{\text{huber}}(y, \hat{y}_{\text{ref}})$ . In the reference-free setting, we use only  $\mathcal{L}_{\text{huber}}(y, \hat{y}_{\text{img}})$ .

## Spica Dataset

The development of supervised metrics for image captioning requires large-scale and diverse datasets in terms of the number of images, annotators, and captioning models. Specifically, a dataset should: (i) contain an extensive collection of human judgments and (ii) include a diverse and large-scale set of images to effectively capture the similarities between images and candidate captions. However, few standard datasets (Aditya et al. 2015; Hodosh et al. 2013; Wada et al. 2024; Matsuda et al. 2024) meet both criteria. The dataset with the largest collection of human judgments (Wada et al. 2024) comprises approximately 131k

Metrics	Ref	Composite		Flickr8K-Ex		Flickr8K-CF		Nebula		FOIL		Test time [hour]
		$\tau_b$	$\tau_c$	$\tau_b$	$\tau_c$	$\tau_b$	$\tau_c$	$\tau_b$	$\tau_c$	1-ref [%]	4-ref [%]	
<b>LLM-free methods (reference-based)</b>												
BLEU (Papineni et al. 2002)	✓	28.3	30.6	30.6	30.8	16.4	8.7	46.5	44.1	66.5	82.6	< 0.01
ROUGE (Lin 2004)	✓	30.0	32.4	32.1	32.3	19.9	10.3	45.8	43.4	71.7	79.3	< 0.01
CIDEr (Vedantam, Zitnick, and Parikh 2015)	✓	34.9	37.7	43.6	43.9	24.6	12.7	51.5	48.8	82.5	90.6	< 0.01
METEOR (Banerjee et al. 2005)	✓	36.0	38.9	41.5	41.8	22.2	11.5	50.2	47.6	78.8	82.6	< 0.01
SPICE (Anderson et al. 2016)	✓	38.8	40.3	51.7	44.9	24.4	12.0	51.5	47.4	75.5	86.1	0.089
RefCLIP-S <sup>†</sup> (Hessel, Holtzman et al. 2021)	✓	51.2	55.4	52.6	53.0	36.4	18.8	53.6	50.8	91.0	92.6	0.014
RefPAC-S <sup>†</sup> (Sarto, Barraco et al. 2023)	✓	53.0	57.3	55.5	55.9	37.6	19.5	54.7	51.9	93.7	94.9	0.023
Polos (Wada et al. 2024)	✓	53.7	57.6	56.1	56.4	37.8	19.5	58.0	55.0	93.3	95.4	0.036
Ref-HICEScore (Zeng et al. 2024a)	✓	53.9	58.7	57.2	57.7	38.2	19.8	-	-	96.4	97.0	-
DENEB <sup>†</sup> (Matsuda et al. 2024)	✓	54.0	57.9	55.6	56.5	38.0	19.6	58.1	55.1	95.1	96.1	0.038
RefPAC-S++ <sup>†</sup> (Sarto, Moratelli et al. 2024)	✓	54.7	59.1	55.3	55.7	37.9	19.6	53.3	50.6	93.5	94.1	0.023
<b>Ours (ViT-B/32)</b>	✓	<b>55.8</b>	<b>60.4</b>	<b>58.2</b>	<b>58.6</b>	<b>38.6</b>	<b>20.0</b>	<b>58.4</b>	<b>55.4</b>	<b>96.5</b>	<b>97.2</b>	0.043
<b>LLM-free methods (reference-free)</b>												
CLIP-S (Hessel, Holtzman et al. 2021)		49.8	53.8	51.1	51.2	34.4	17.7	50.5	47.9	87.2	87.2	< 0.01
PAC-S <sup>†</sup> (Sarto, Barraco et al. 2023)		51.5	55.7	53.9	54.3	36.0	18.6	51.0	48.3	89.9	89.9	0.013
HICEScore (Zeng et al. 2024a)		53.1	57.9	55.9	56.4	37.2	19.2	-	-	93.1	93.1	-
PAC-S++ <sup>†</sup> (Sarto, Moratelli et al. 2024)		53.9	58.3	54.1	54.5	37.0	19.1	50.5	47.9	90.2	90.2	0.013
BLIP2Score (Zeng et al. 2024b)		<b>56.9</b>	<b>61.5</b>	52.2	52.5	36.7	19.0	53.0	50.7	94.3	94.3	0.020
<b>Ours (ViT-B/32)</b>		<b>54.0</b>	<b>58.4</b>	<b>56.2</b>	<b>56.6</b>	<b>37.8</b>	<b>19.5</b>	<b>55.9</b>	<b>53.0</b>	<b>96.7</b>	<b>96.7</b>	0.043
<b>LLM-based methods</b>												
CLAIR <sup>1</sup> (Chan, Petryk et al. 2023)	✓	-	61.0	58.3	48.8	38.2	17.0	-	-	-	93.6	8.3
FLEUR (Lee et al. 2024)		-	63.5	-	53.0	38.6	-	-	-	96.8	96.8	3.7
Ref-FLEUR (Lee et al. 2024)	✓	-	64.2	-	51.9	38.8	-	-	-	97.3	98.4	4.0
HiFiScore (Yao et al. 2024)		-	65.7	-	58.4	-	-	-	-	-	-	-
Ref-HiFiScore (Yao et al. 2024)	✓	-	65.8	-	58.4	-	-	-	-	-	-	-
G-VEval (Tong, He et al. 2024)		-	-	61.5	59.7	38.7	20.2	-	-	-	-	11
Ref-G-VEval (Tong, He et al. 2024)	✓	-	-	60.5	58.7	38.2	19.9	-	-	97.8	98.4	11
EXPERT (Kim et al. 2025)		-	65.0	-	56.7	39.3	-	-	54.9	-	-	-

Table 1: Quantitative comparison with baseline metrics. The column “Ref” indicates whether the method uses reference captions. Bold font indicates the best values and underline indicates the second best values. “-” indicates either non executable code or unavailable data. “ $\tau_b$ ” and “ $\tau_c$ ” represent Kendall’s  $\tau_b$  and  $\tau_c$  correlation coefficients, respectively. “Test time” refers to the total inference time for evaluating the test sets of COCO (Lin et al. 2014), nocaps (Agrawal, Desai et al. 2019), and TextCaps (Sidorov, Hu et al. 2020). Metrics marked with <sup>†</sup> use ViT-B/32 as the backbone for a fair comparison.

human judgments but contains only 13k images. As noted in (Matsuda et al. 2024), this imbalance could potentially lead to suboptimal evaluation of various types of images. Similarly, Nebula (Matsuda et al. 2024) has the largest number of unique images but only 32k human judgments, which can result in suboptimal alignment with human judgments.

To address these gaps, we constructed the Spica dataset, which includes (i) a large number of human judgments and (ii) a diverse and extensive collection of images. The Spica dataset comprises 333,397 human judgments collected from 2,360 annotators and 75,535 unique images. Our dataset stands out with its significantly larger number of human judgments and greater diversity of both images and annotators. Specifically, our dataset includes 2.5 times the number of human judgments as the Polaris dataset (Wada et al. 2024), the largest existing dataset in terms of human judgments. Moreover, our dataset contains 2.3 times as many unique images as the Nebula dataset (Matsuda et al. 2024), which currently has the highest number of unique images. To generate candidate captions, we employed the ten image

captioning models. The criteria of model selection, the statistical information and details of our dataset can be found in the Appendix.

## Experiments

To evaluate the correlation between the metric and human judgments on both in-domain and out-of-domain samples, we used the Composite (Aditya et al. 2015), Flickr8K-Expert (Hodosh et al. 2013), Flickr8K-CF, and Nebula (Matsuda et al. 2024) datasets. Note that we corrected the annotation errors found in the Nebula dataset. Moreover, to assess robustness against hallucination, we conducted comparative experiments with the FOIL dataset (Shekhar et al. 2017). We selected these benchmarks because they are standard in this field. Details of the baselines are provided in the Appendix.

<sup>1</sup>Following standard practice (Tong, He et al. 2024; Lee et al. 2024), we report the scores of CLAIR as reproduced in (Tong, He et al. 2024; Lee et al. 2024), because the originally reported results exhibit a disparity in the calculation method compared to other metrics (<https://github.com/DavidMChan/clair/issues/2>).

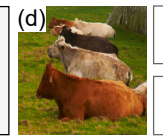
	<p>Candidate "a black dog sitting on a dog bed with a banana in its mouth"</p> <p>Reference "a dog on a lawn chair with a banana in its mouth"</p>	<p><b>Human</b> <b>0.90</b></p> <p><b>Ours</b> <b>0.87</b></p> <p>DENE B 0.67</p> <p>RefPAC-S++ 0.66</p>		<p>Candidate "a white toilet"</p> <p>Reference "Pots and covered dishes setting a stove in a kitchen"</p>	<p><b>Human</b> <b>0.00</b></p> <p><b>Ours</b> <b>0.08</b></p> <p>DENE B 0.42</p> <p>RefPAC-S++ 0.46</p>
	<p>Candidate "a man standing in the snow"</p> <p>Reference —</p>	<p><b>Human</b> <b>0.75</b></p> <p><b>Ours</b> <b>0.81</b></p> <p>BLIP2-S 0.38</p> <p>PAC-S++ 0.53</p>		<p>Candidate "the elephant is brown"</p> <p>Reference —</p>	<p><b>Human</b> <b>0.00</b></p> <p><b>Ours</b> <b>0.21</b></p> <p>BLIP2-S 0.21</p> <p>PAC-S++ 0.28</p>

Figure 3: Qualitative results on the Nebula dataset. Cases (a) and (b) show successful cases in the reference-based setting, while Case (c) highlights successful sample in the reference-free setting. Case (d) shows a failure case in the reference-free setting.

## Quantitative Results

**Human correlation.** Table 1 presents the quantitative comparison results between the baselines and our proposed metric on the Composite, Flickr8K-Expert, Flickr8K-CF, and Nebula datasets. We employed Kendall’s  $\tau_b$  and  $\tau_c$  correlation coefficients, as they are standard for evaluation in this field. In the reference-based setting, Pearl achieved  $\tau_b$  scores of 55.8, 58.2, 38.6, and 58.4 and  $\tau_c$  scores of 60.4, 58.6, 20.0 and 55.4 on the Composite, Flickr8K-Expert, Flickr8K-CF, and Nebula datasets, respectively. These results indicate that Pearl outperformed the existing LLM-free baseline metrics by margins of 1.1, 1.0, 0.4 and 0.3 points for  $\tau_b$  and 1.3, 0.9, 0.2, and 0.3 points for  $\tau_c$ . Pearl achieved an average increase of 1.1 points in  $\tau_b$  and 0.93 in  $\tau_c$  over Ref-HICEScore, the previous SOTA baseline metrics. In comparison, the average improvement of Ref-HICEScore over RefPAC-S++, the second best previous metrics, was only 0.47 and 0.60 in  $\tau_b$  and  $\tau_c$ , respectively. These results indicate that Pearl yielded substantial improvements.

In the reference-free setting, our method achieved  $\tau_b$  of 56.2, 37.8, and 55.9, and  $\tau_c$  of 56.6, 19.5, and 53.0 on the Flickr8K-CF, Flickr8K-Expert, and Nebula datasets, respectively. These results indicate improvements of 0.3, 0.6, and 2.9 points for  $\tau_b$ , and 0.2, 0.3, and 2.3 points for  $\tau_c$  over the previous LLM-free SOTA baseline metrics, respectively.

**Sensitivity to hallucination.** Table 1 shows the performance of the proposed metric and the baseline metrics on the FOIL dataset. In the reference-based setting, Pearl achieved SOTA performance among LLM-free metrics, with scores of 96.5% in the one-reference setting and 97.2% in the four-references setting. Moreover, in the reference-free setting, our metric also achieved a SOTA performance of 96.7% among LLM-free metrics, representing an improvement of 2.4 points over existing LLM-free metrics. These results suggest that our metric is robust even against hallucinations.

**Inference time.** The rightmost column of Table 1 shows the total inference time for evaluating the test sets of COCO (Lin et al. 2014), nocaps (Agrawal, Desai et al. 2019), and TextCaps(Sidorov, Hu et al. 2020), which are the standard benchmarks for image captioning (McKinzie et al. 2024; Xiao et al. 2024). All measurements were taken on a system equipped with a GeForce RTX 3090 and an Intel Core i9-10900KF. The inference times for recent LLM-free

metrics, RefCLIP-S and RefPAC-S, were 0.014 and 0.023 hours, respectively. Pearl showed an inference time of 0.043 hours, suggesting that Pearl is comparable in terms of inference speed. In contrast, LLM-based metrics such as CLAIR and FLEUR exhibited significantly longer inference times of 8.3 and 3.7 hours, respectively, which makes them at least 85 times slower than Pearl.

## Qualitative Results

**Successful cases.** Fig. 3 shows successful cases of Pearl on the Nebula dataset. In the figure, Cases (a) and (b) show successful cases in the reference-based setting, while Case (c) displays a successful case in the reference-free setting.

In Case (a), the human judgment was 0.90 because  $x_{\text{cand}}$  appropriately describes the image. Ref-CLIPS and Ref-PAC-S++ incorrectly evaluated this sample with scores of 0.67 and 0.66, respectively, whereas Pearl appropriately evaluated it with a value of 0.87. Similarly, in Case (b), Pearl yielded the score most aligned with human judgment.

Case (c) shows a successful sample in the reference-free setting. The human judgment was 0.75 because the caption only partially describes the image. Both PAC-S++ and BLIP2-S incorrectly evaluated the sample with scores of 0.53 and 0.38, respectively, whereas Pearl assigned a score of 0.81, which more closely aligned with the human judgment.

**Failure case.** Case (d) in Fig. 3 illustrates a failure case in the reference-free setting. In this sample,  $x_{\text{cand}}$  was incorrectly described as “The elephant is brown,” which does not correspond to  $x_{\text{img}}$ . This discrepancy resulted in a human judgment score of 0.00. However, our proposed metric evaluated this sample with a score of 0.21. Similarly, PAC-S++ and BLIP2-S assigned the sample scores of 0.28 and 0.21, respectively, demonstrating discrepancies as well. Given that the subject (i.e., “elephant”) is misidentified in this example, the presence of the adjective “brown” should not contribute to an increased score. However, these metrics include color information when computing similarity; therefore, we hypothesize that the failure occurs because even if the core part (e.g., the subject identification) is incorrect, the presence of correct color information leads to a score increase.

Moreover, to examine additional failure cases, we analyzed the 100 samples with the greatest absolute differences between  $\hat{y}$  and  $y$ . For details of the analysis, see Appendix.

Metric	ARSM	Image Encoder			Text Encoder	Composite	Flickr8K-Ex	Flickr8K-CF	Nebula
		CLIP	BLIP-2	BEiT-3					
(i)	none	✓	✓	✓	✓	30.9	31.2	17.4	41.7
(ii)	initial	✓	✓	✓	✓	54.3	58.2	38.5	52.5
(iii)	RUSE-type	✓	✓	✓	✓	59.5	56.7	37.3	50.3
(iv)	adaptive	✓	✓	✓		51.9	56.0	37.3	52.0
(v)	adaptive		✓	✓	✓	55.5	54.2	35.8	53.9
(vi)	adaptive	✓		✓	✓	59.0	57.3	38.0	54.0
(vii)	adaptive	✓	✓		✓	59.9	58.3	38.4	53.9
(viii)	adaptive	✓	✓	✓	✓	<b>60.4</b>	<b>58.6</b>	<b>38.6</b>	<b>55.4</b>

Table 2: Results of ARSM ablation and feature extractor ablation in reference-based setting. “ $\tau_b$ ” and “ $\tau_c$ ” represents the Kendall’s  $\tau_b$  and  $\tau_c$  correlation coefficient, respectively. Results for reference-free setting are in the Appendix.

Metrics	Training Dataset	Com	Ex	CF
		$\tau_c$	$\tau_c$	$\tau_b$
(a) DENEB	Nebula	57.9	56.5	38.0
(b) DENEB	Spica	58.6	56.9	38.2
(c) Pearl	Nebula	59.2	57.7	37.9
(d) Pearl	Spica	<b>60.4</b>	<b>58.6</b>	<b>38.6</b>

Table 3: Results of the Spica ablation. “Com”, “EX” and “CF” represent Composite, Flickr8K-EX and Flickr8K-CF.

## Ablation Study

We conducted ablation studies to assess the impact of each module and Spica dataset. Tables 2 and 3 show the results of the ablation studies. Results in the reference-free setting are provided in the Appendix.

**ARSM ablation.** We investigated the contribution of ARSM, which learns features, in three different ways: by removing it, freezing its parameters at their initial values, and replacing it with a non learnable RUSE-type similarity. Table 2 shows that Metric (i) yielded correlation coefficients of 30.9, 31.2, 17.4, and 41.7 for Composite, Flickr8K-Expert, Flickr8K-CF, and Nebula, respectively. These values decreased by 29.5, 27.4, 21.2, and 13.7 points compared with those of Metric (viii).

Moreover, Metric (iii), a version where ARSM was replaced with a non-learnable RUSE-type similarity, yielded correlation coefficients of 59.5, 56.7, 37.3, and 50.3 for Composite, Flickr8K-Expert, Flickr8K-CF, and Nebula, respectively. These values decreased by 0.9, 1.9, 1.3, and 5.1 points compared to Metric (viii). These results indicate that ARSM was effective at extracting significant features for evaluation and significantly contributed to performance.

**Feature extractor ablation.** We investigated the contribution of image and text encoders by removing CLIP, BLIP-2, BEiT-3, and Stella. Table 2 demonstrates that Metric (iv), which corresponds to Pearl without the Stella encoder, achieved correlation coefficients of 51.9, 56.0, 37.3, and 52.0 on Composite, Flickr8K-Expert, Flickr8K-CF, and Nebula, respectively. Compared to the original Pearl (viii),

these scores decreased by 8.5, 2.6, 1.3, and 3.4 points, respectively, highlighting the significant contribution of Stella to performance in the reference-based setting.

Moreover, Table 2 shows that Metric (v), which corresponds to Pearl without the CLIP encoder, yielded correlation coefficients of 55.5, 54.2, 35.8 and 53.9 on Composite, Flickr8K-Expert, Flickr8K-CF, and Nebula, respectively. Compared with those of the original Pearl (viii), these values decreased by 4.9, 4.4, 2.8 and 1.5 points. These results indicate that CLIP significantly contributed to the performance.

However, they do not indicate that CLIP is the sole contributor to Pearl’s performance. To further investigate this, we conducted an ablation study where all encoders except CLIP were removed. Details are provided in the Appendix.

**Spica Ablation.** We evaluated the effectiveness of the Spica dataset by training the existing supervised metric on Spica. We compared DENEB (Matsuda et al. 2024) because it was the previous SOTA among supervised LLM-free metrics. As shown in Table 3, DENEB achieved better performance when trained on Spica (b) compared to when trained on Nebula (a), which is their original training dataset. These results indicate the versatility of Spica for supervised metrics. Moreover, comparing Pearl trained on Nebula (c) with the original model (d) highlights the contribution of the Spica dataset to overall performance. These indicate that Spica provided effective data for training supervised metrics.

## Conclusion

We focused on the automatic evaluation for image captioning. Our contributions are as follows: (i) we proposed Pearl, a supervised metric for reference-flexible settings, (ii) we introduced Img-GEM and Ref-GEM to handle image-caption and caption-caption similarities, (iii) we introduced ARSM, which learns rich similarity representations, (iv) we constructed Spica, a dataset with diverse images and extensive human judgments, and (v) we achieved SOTA performance on standard benchmarks within LLM-free metrics.

The proposed metric performed well on standard benchmarks, although limitations remain. Our error analysis revealed that Pearl assigned incorrect scores to captions that lacked descriptiveness. Details of the analysis are provided in the Appendix.

## Acknowledgments

This work was supported by a grant from Apple, Inc. Any views, opinions, findings, and conclusions or recommendations expressed in this material are those of the authors and should not be interpreted as reflecting the views, policies, or position, either expressed or implied, of Apple, Inc. This work was also partially supported by JSPS KAKENHI Grant Number 23K28168 and JST Moonshot.

## References

Aditya, S.; et al. 2015. From Images to Sentences through Scene Description Graphs using Commonsense Reasoning and Knowledge. *arXiv preprint arXiv:1511.03292*.

Agrawal, H.; Desai, K.; et al. 2019. nocaps: Novel Object Captioning at Scale. In *ICCV*, 8948–8957.

An, N. M.; Kim, E.; Kang, W. J.; Kim, S.; et al. 2025. Can LVLMs and Automatic Metrics Capture Underlying Preferences of Blind and Low-Vision Individuals for Navigational Aid? *arXiv preprint arXiv:2502.14883*.

Anderson, P.; Fernando, B.; Johnson, M.; et al. 2016. SPICE: Semantic Propositional Image Caption Evaluation. In *ECCV*, 382–398.

Banerjee, S.; et al. 2005. METEOR: An Automatic Metric for MT Evaluation with Improved Correlation with Human Judgments. In *ACL*, 65–72.

Chan, D.; Petryk, S.; et al. 2023. CLAIR: Evaluating Image Captions with Large Language Models. In *EMNLP*, 13638–13646.

Chung, H.; Hou, L.; Longpre, S.; Zoph, B.; Tay, Y.; et al. 2022. Scaling Instruction-Finetuned Language Models. *arXiv preprint arXiv:2210.11416*.

Cornia, M.; Stefanini, M.; Baraldi, L.; et al. 2020. Meshed-Memory Transformer for Image Captioning. In *CVPR*, 10578–10587.

Dosovitskiy, A.; Beyer, L.; Kolesnikov, A.; et al. 2021. An Image is Worth 16x16 Words: Transformers for Image Recognition at Scale. In *ICLR*.

Feinglass, J.; and Yang, Y. 2021. SMURF: SeMantic and linguistic UndeRstanding Fusion for Caption Evaluation via Typicality Analysis. In *IJCNLP*, 2250–2260.

Hessel, J.; Holtzman, A.; et al. 2021. CLIPScore: A Reference-free Evaluation Metric for Image Captioning. In *EMNLP*, 7514–7528.

Hodosh, M.; et al. 2013. Framing Image Description as a Ranking Task: Data, Models and Evaluation Metrics. *JAIR*, 47: 853–899.

Kasai, J.; Sakaguchi, K.; Dunagan, L.; Morrison, J.; et al. 2022. Transparent Human Evaluation for Image Captioning. In Carpuat, M.; de Marneffe, M.-C.; and Meza Ruiz, I. V., eds., *NAACL*, 3464–3478.

Kim, H.; Kim, S.; Jeong, J.; Cho, Y.; and Cho, S. 2025. EXPERT: An Explainable Image Captioning Evaluation Metric with Structured Explanations. In *ACL*, 26642–26657.

Lee, H.; Yoon, S.; et al. 2021. UMIC: An Unreferenced Metric for Image Captioning via Contrastive Learning. In *ACL*, 220–226.

Lee, H.; et al. 2020. ViLBERTScore: Evaluating Image Caption Using Vision-and-Language BERT. In *Evaluation and Comparison of NLP Systems*, 34–39.

Lee, Y.; et al. 2024. FLEUR: An Explainable Reference-Free Evaluation Metric for Image Captioning Using a Large Multimodal Model. In *ACL*, 3732–3746.

Li, J.; et al. 2022. BLIP: Bootstrapping Language-Image Pre-training for Unified Vision-Language Understanding and Generation. In *ICML*, 12888–12900.

Li, J.; et al. 2023. BLIP-2: Bootstrapping Language-Image Pre-training with Frozen Image Encoders and Large Language Models. In *ICML*, 19730–19742.

Lin, C. 2004. ROUGE: A Package For Automatic Evaluation Of Summaries. In *ACL*, 74–81.

Lin, T.; Maire, M.; Belongie, S.; Bourdev, L.; Girshick, R.; et al. 2014. Microsoft COCO: Common Objects in Context. In *ECCV*, 740–755.

Liu, H.; Li, C.; Li, Y.; and Lee, Y. J. 2024. Improved Baselines with Visual Instruction Tuning. In *CVPR*, 26296–26306.

Liu, H.; Li, C.; et al. 2023. Visual Instruction Tuning. In *NeurIPS*, 34892–34916.

Lu, J.; et al. 2019. ViLBERT: Pretraining Task-Agnostic Visiolinguistic Representations for Vision-and-Language Tasks. In *NeurIPS*, 13–23.

Matsuda, K.; Wada, Y.; Hirano, S.; Otsuki, S.; and Sugiura, K. 2025. VELA: An LLM-Hybrid-as-a-Judge Approach for Evaluating Long Image Captions. In *EMNLP*, 8691–8707.

Matsuda, K.; et al. 2024. DENEB: A Hallucination-Robust Automatic Evaluation Metric for Image Captioning. In *ACCV*, 3570–3586.

McKinzie, B.; Gan, Z.; Fauconnier, J.-P.; Dodge, S.; Zhang, B.; Dufter, P.; Shah, D.; Du, X.; Peng, F.; Belyi, A.; et al. 2024. MM1: methods, analysis and insights from multi-modal LLM pre-training. In *ECCV*, 304–323. Springer.

Navigli, R.; Conia, S.; and Ross, B. 2023. Biases in large language models: origins, inventory, and discussion. *ACM*, 15(2): 1–21.

Ohi, M.; et al. 2024. HarmonicEval: Multi-modal, Multi-task, Multi-criteria Automatic Evaluation Using a Vision Language Model. *arXiv preprint arXiv:2412.14613*.

Panickssery, A.; Bowman, S. R.; and Feng, S. 2024. LLM Evaluators Recognize and Favor Their Own Generations. In *NeurIPS*.

Papineni, K.; Roukos, S.; Ward, T.; and Zhu, W. 2002. BLEU: a Method for Automatic Evaluation of Machine Translation. In *ACL*, 311–318.

Radford, A.; Kim, J. W.; Hallacy, C.; et al. 2021. Learning Transferable Visual Models from Natural Language Supervision. In *ICML*, 8748–8763.

Rei, R.; Stewart, C.; Farinha, A.; and Lavie, A. 2020. COMET: A Neural Framework for MT Evaluation. In *EMNLP*, 2685–2702.

Sarto, S.; Barraco, M.; et al. 2023. Positive-Augmented Contrastive Learning for Image and Video Captioning Evaluation. In *CVPR*, 6914–6924.

Sarto, S.; Cornia, M.; et al. 2024. BRIDGE: Bridging Gaps in Image Captioning Evaluation with Stronger Visual Cues. In *ECCV*, 70–87.

Sarto, S.; Moratelli, N.; et al. 2024. Positive-Augmented Contrastive Learning for Vision-and-Language Evaluation and Training. *arXiv preprint arXiv:2410.07336*.

Shekhar, R.; Pezzelle, S.; Klimovich, Y.; et al. 2017. FOIL it! Find One Mismatch Between Image and Language caption. In *ACL*, 255–265.

Shimanaka, H.; et al. 2018. RUSE: Regressor Using Sentence Embeddings for Automatic Machine Translation Evaluation. In *WMT*, 751–758.

Sidorov, O.; Hu, R.; et al. 2020. TextCaps: a Dataset for Image Captioning with Reading Comprehension. In *ECCV*, 742–758.

Suganuma, M.; Okatani, T.; et al. 2022. GRIT: Faster and Better Image Captioning Transformer Using Dual Visual Features. In *ECCV*, 167–184.

Tong, T. C.; He, S.; et al. 2024. G-VEval: A Versatile Metric for Evaluating Image and Video Captions Using GPT-4o. *arXiv preprint arXiv:2412.13647*.

Vedantam, R.; Zitnick, L.; and Parikh, D. 2015. CIDEr: Consensus-based Image Description Evaluation. In *CVPR*, 4566–4575.

Wada, Y.; Kaneda, K.; and Sugiura, K. 2023. JaSPICE: Automatic Evaluation Metric Using Predicate-Argument Structures for Image Captioning Models. In *CoNLL*, 424–435.

Wada, Y.; et al. 2024. Polos: Multimodal Metric Learning from Human Feedback for Image Captioning. In *CVPR*, 13559–13568.

Wang, J.; Yang, Z.; Hu, X.; Li, L.; Lin, K.; Gan, Z.; et al. 2022a. GIT: A Generative Image-to-text Transformer for Vision and Language. *TMLR*.

Wang, P.; et al. 2022b. OFA: Unifying Architectures, Tasks, and Modalities Through a Simple Sequence-to-sequence Learning Framework. In *ICML*, 23318–23340.

Wang, W.; Bao, H.; Dong, L.; Bjorck, J.; Peng, Z.; Liu; et al. 2023. Image as a foreign language: Beit pretraining for vision and vision-language tasks. In *CVPR*, 19175–19186.

Xiao, B.; Wu, H.; Xu, W.; Dai, X.; Hu, H.; Lu, Y.; Zeng, M.; et al. 2024. Florence-2: Advancing a unified representation for a variety of vision tasks. In *CVPR*, 4818–4829.

Yao, Z.; et al. 2024. HiFi-Score: Fine-Grained Image Description Evaluation with Hierarchical Parsing Graphs. In *ECCV*, 441–458.

Yuan, W.; Neubig, G.; et al. 2021. BARTScore: Evaluating Generated Text as Text Generation. In *NeurIPS*, volume 34, 27263–27277.

Zeng, Z.; Sun, J.; Zhang, H.; Wen, T.; Su, Y.; Xie, Y.; et al. 2024a. HICEScore: A Hierarchical Metric for Image Captioning Evaluation. In *ACM, MM '24*, 866–875.

Zeng, Z.; Xie, Y.; Zhang, H.; Chen, C.; Chen, B.; et al. 2024b. MeaCap: Memory-Augmented Zero-shot Image Captioning. In *CVPR*, 14100–14110.

Zhang, D.; Li, J.; Zeng, Z.; and Wang, F. 2024. Jasper and Stella: distillation of SOTA embedding models. *arXiv preprint arXiv:2412.19048*.

Zhang, P.; Li, X.; Hu, X.; et al. 2021. VinVL: Revisiting Visual Representations in Vision-language Models. In *CVPR*, 5579–5588.

Zhang, S.; Roller, S.; Goyal, N.; Artetxe, M.; et al. 2022. OPT: Open Pre-trained Transformer Language Models. *arXiv preprint arXiv:2205.01068*.

Zhang, T.; Kishore, V.; Wu, F.; Weinberger, K.; and Artzi, Y. 2020. BERTScore: Evaluating Text Generation with BERT. In *ICLR*.

## Appendix A: Additional Related Works

**Benchmarks.** Several benchmarks have been proposed for image captioning metrics (Hodosh et al. 2013; Aditya et al. 2015; Wada et al. 2024; Matsuda et al. 2024; Shekhar et al. 2017; An et al. 2025). Flickr8K-Expert (Hodosh et al. 2013) and Flickr8K-CF (Hodosh et al. 2013) provide human judgments for candidate captions associated with 1,000 images from the Flickr8K test set. Flickr8K-Expert and Flickr8K-CF contain 5,822 and 47,830 candidate captions, respectively. In Composite (Aditya et al. 2015), each image is paired with two candidate captions and one reference. Composite has 3,996 unique images and 11,985 human judgments for each candidate caption. The Polaris dataset (Wada et al. 2024) contains over 131k human judgments for the captions generated for approximately 14k images, making it the largest among similar datasets in terms of human judgments. Similarly, Nebula (Matsuda et al. 2024) is the largest in terms of image count, containing approximately three times as many images as Polaris. In this study, we constructed Spica, a significantly larger human-annotated dataset for image captioning metrics than previous ones. Our dataset contains 2.5 times the number of human judgments that Polaris has and 2.3 times the number of images that Nebula has (see the *Spica Dataset* section).

## Appendix B: Datasets

### Spica Dataset

**Image captioning models.** We employ the following standard image captioning models to generate candidate captions: VinVL (Zhang et al. 2021), GRIT (Suganuma, Okatani et al. 2022),  $\mathcal{M}^2$ -Transformer (Cornia et al. 2020), BLIP (Li et al. 2022), GIT (Wang et al. 2022a), OFA (Wang et al. 2022b), and BLIP-2 (Li et al. 2023). For BLIP, we utilized two versions that employ ViT-B and ViT-L (Dosovitskiy et al. 2021) as their image encoders. Similarly, for BLIP-2, we employed two variants that use Flan-T5 (Chung et al. 2022) and OPT (Zhang et al. 2022) as the LLMs. We selected these models in terms of their providing organizations (e.g., Alibaba, Microsoft, Academia) and release years, in order to minimize the model bias.

**Image diversity.** To analyze the diversity of images in our dataset, we measure semantic coverage based on the geometric coverage in the CLIP image embedding space. Specifically, we computed the proportion of the convex hull volume formed by each dataset (Flickr8k-CF (Hodosh et al. 2013), Flickr8k-EX, Composite (Aditya et al. 2015), and Nebula (Matsuda et al. 2024)) to the entire OpenImages. The results show that Flickr8k-CF, Flickr8k-Expert, Composite, Nebula, and Spica cover 25.3%, 25.3%, 50.3%, 85.4%, and 91.6% of the OpenImages hull. These results demonstrate that Spica provided more diverse images than other standard benchmarks (Hodosh et al. 2013; Aditya et al. 2015; Matsuda et al. 2024).

**Annotation bias.** Spica was designed to exhibit low bias in the distribution of human judgments, comparable to those of Composite and Polaris. By contrast, in Flickr8k-CF and Flickr8k-EX, 88% and 55% of the scores are concentrated at

Dataset	Annotators	Unique images	Human judgments
CapEval1K	5	250	1,000
THumB	4	500	2,500
MMHE	5	100	4,500
Composite	–	3,996	11,985
flickr8k-EX	21	1,000	16,992
Nebula	805	32,978	32,978
flickr8K-CF	–	1,000	47,830
Polaris	550	13,691	131,020
<b>Spica (Ours)</b>	<b>2,360</b>	<b>75,535</b>	<b>333,397</b>

Table 4: Comparison between Spica and the standard datasets. Spica stands out with its significantly larger number of human judgments and greater diversity of both images and annotators.

0.0, respectively. Moreover, Krippendorff’s  $\alpha$  for the inter-annotator agreement was 0.44, which is higher than that of standard datasets (e.g. CapEval1k (Lee, Yoon et al. 2021)).

**Annotations.** We followed standard practices in this field during the annotation process (Aditya et al. 2015; Kasai et al. 2022; Lee, Yoon et al. 2021; Wada et al. 2024; Matsuda et al. 2024). Human judgments were collected on a five-point scale to evaluate the appropriateness of candidates in relation to the given images and references. Annotators were instructed to assess captions across three dimensions: *fluency*, *relevance*, and *descriptiveness*. To ensure data reliability, annotations from evaluators displaying suspicious behavior, such as abnormally short response times or consistently uniform ratings, were excluded. We normalized the human judgments from a five-point scale to the range  $[0, 1]$ .

**Statistics.** The statistics of the Spica dataset are summarized in Table 4. The total number of references in Spica is 1,128,933, with a vocabulary size of 36,947, a total word count of 11,278,014, and an average sentence length of 10.0 words. The total number of candidates is 333,397, with a vocabulary size of 15,697, a total word count of 2,936,768, and an average sentence length of 8.8 words. We divided the Spica dataset into training, validation, and test sets, containing 296,149, 3,000, and 3,287 samples, respectively. We used the training set, validation set, and test set to train the model, tune the hyperparameters, and evaluate the model’s performance, respectively.

### Human Performance on Nebula Dataset

To evaluate human performance, we conducted a subject experiment on the Nebula dataset. We opted for the Nebula dataset because of its reliability in ground-truth judgments; the ground-truth judgments are given by an average of four annotators per sample, a higher number than those of other standard datasets (Aditya et al. 2015; Hodosh et al. 2013). First, we randomly selected 330 samples from the test set. Next, four subjects provided scores for these samples in a reference-free setting. We then calculated Kendall’s  $\tau$  for each subject’s judgments against the ground truth and com-

Metrics	Ref	Composite		Flickr8K-Ex		Flickr8K-CF		Nebula		FOIL		Test time
		$\tau_b$	$\tau_c$	$\tau_b$	$\tau_c$	$\tau_b$	$\tau_c$	$\tau_b$	$\tau_c$	1-ref [%]	4-ref [%]	
<b>LLM-free (reference-based)</b>												
BERTScore (Zhang et al. 2020)	✓	30.2	30.1	37.8	46.7	22.8	11.5	47.5	47.1	88.6	92.1	0.040
BARTScore (Yuan, Neubig et al. 2021)	✓	30.4	43.5	32.5	37.8	24.3	10.3	47.4	45.0	85.3	91.1	0.68
SPARCS (Feinglass and Yang 2021)	✓	41.4	43.1	43.8	48.1	25.2	13.0	53.9	50.0	86.0	92.1	< 0.01
<b>Ours (ViT-B/32)</b>	✓	<b>55.8</b>	<b>60.4</b>	<b>58.2</b>	<b>58.6</b>	<b>38.6</b>	<b>20.0</b>	<b>58.4</b>	<b>55.4</b>	<b>96.5</b>	<b>97.2</b>	0.043
<b>LLM-free (reference-free)</b>												
BRIDGE (Sarto, Cornia et al. 2024)		52.9	57.2	55.4	55.8	36.3	19.0	-	-	93.0	93.0	-
<b>Ours (ViT-B/32)</b>		<b>54.0</b>	<b>58.4</b>	<b>56.2</b>	<b>56.6</b>	<b>37.8</b>	<b>19.5</b>	<b>55.9</b>	<b>53.0</b>	<b>96.7</b>	<b>96.7</b>	0.043

Table 5: Additional quantitative comparison with baselines. The column “Ref” indicates whether the method uses reference captions. Bold font indicates the best values. “-” indicates either non executable code or unavailable data. “ $\tau_b$ ” and “ $\tau_c$ ” represent Kendall’s  $\tau_b$  and  $\tau_c$  correlation coefficients, respectively. “Test time” refers to the total inference time for evaluating the test sets of COCO (Lin et al. 2014), nocaps (Agrawal, Desai et al. 2019), and TextCaps (Sidorov, Hu et al. 2020).

Metric	ARSM	Image Encoder			Text Encoder	Composite	Flickr8K-Ex	Flickr8K-CF	Nebula
		CLIP	BLIP-2	BEiT-3					
(i)	none	✓	✓	✓	✓	30.7	30.4	16.7	42.3
(ii)	initial	✓	✓	✓	✓	53.0	56.2	37.6	52.2
(iii)	RUSE-type	✓	✓	✓	✓	58.2	55.4	36.7	49.3
(iv)	adaptive	✓	✓	✓	✓	<b>58.4</b>	<b>56.6</b>	<b>37.8</b>	<b>53.0</b>
(v)	adaptive		✓	✓	✓	55.0	53.5	35.5	51.5
(vi)	adaptive	✓		✓	✓	58.3	56.7	37.7	52.6
(vii)	adaptive	✓	✓		✓	58.4	56.3	37.6	52.4
(viii)	adaptive	✓	✓	✓	✓	<b>58.4</b>	<b>56.6</b>	<b>37.8</b>	<b>53.0</b>

Table 6: Ablation studies for reference-free setting. “ $\tau_b$ ” and “ $\tau_c$ ” represents the Kendall’s  $\tau_b$  and  $\tau_c$  correlation coefficient, respectively.

puted the average across all subjects to measure human performance. The results showed that the coefficients for the human performance were 63.3 and 63.0 for  $\tau_b$  and  $\tau_c$ , respectively.

## Appendix C: Experimental Setup

**Baselines.** In the reference-based setting, we employed BLEU (Papineni et al. 2002), ROUGE (Lin 2004), METEOR (Banerjee et al. 2005), CIDEr (Vedantam, Zitnick, and Parikh 2015), and SPICE (Anderson et al. 2016) as baseline metrics, as these are standard metrics for image captioning tasks. We also employed BERTScore (Zhang et al. 2020), BARTScore (Yuan, Neubig et al. 2021), Ref-CLIPScore (Hessel, Holtzman et al. 2021), SPARCS (Feinglass and Yang 2021), Ref-PAC-S (Sarto, Barraco et al. 2023), Ref-PAC-S++ (Sarto, Moratelli et al. 2024), Ref-HICEScore (Zeng et al. 2024a), Polos (Wada et al. 2024), DENEB (Matsuda et al. 2024), FLEUR (Lee et al. 2024), G-VEval (Tong, He et al. 2024), and HiFiScore (Yao et al. 2024) as baseline metrics, since they are representative reference-based metrics.

In the reference-free setting, we adopted CLIP-S (Hessel, Holtzman et al. 2021), HICEScore (Zeng et al. 2024a), PAC-S++ (Sarto, Moratelli et al. 2024), BRIDGE (Sarto, Cornia et al. 2024), BLIP2-Score (Zeng et al. 2024b), FLEUR (Lee et al. 2024), HiFiScore (Yao et al. 2024), and EXPERT (Kim et al. 2025) as baselines because they are representative

reference-free metrics. Note that CLAIR (Chan, Petryk et al. 2023), FLEUR (Lee et al. 2024), G-VEval (Tong, He et al. 2024), HiFiScore (Yao et al. 2024), and EXPERT (Kim et al. 2025) are LLM-based metrics, while the others are LLM-free.

**Implementation details.** We adopted the Adam optimizer ( $\beta_1 = 0.9$ ,  $\beta_2 = 0.999$ ) for training, with a learning rate of  $10^{-5}$ , a batch size of 16, and max number of epochs, 5. The number of CNN layers in HadamardNet was set to 8. The VSS submodule used 2 Transformer layers and 1 Q-Former layer. We employed early stopping during training based on Kendall’s  $\tau_c$ . Specifically, the value of  $\tau_c$  was measured on the validation set at the end of each epoch. Training was stopped when the following condition was satisfied:  $\tau_c^{(t)} \leq \tau_c^{(t-1)}$ , where  $\tau_c^{(t)}$  denotes the value of  $\tau_c$  at the end of epoch  $t$  on the validation set. After training, the model with the highest  $\tau_c$  value on the validation set was selected, and its performance was evaluated on the test set.

Following previous works (Hessel, Holtzman et al. 2021; Sarto, Barraco et al. 2023; Wada et al. 2024; Matsuda et al. 2024; Lee et al. 2024; Yao et al. 2024), all experiments were reported based on a single run. Our model had approximately 119 million trainable parameters. We trained our model on a GeForce RTX 3090 with 24GB of memory and an Intel Core i9 12900K with 64GB of memory. The training phase was completed in approximately 4.5 hours,

Metric	ARSM	Image Encoder			Text Encoder	Composite	Flickr8K-Ex	Flickr8K-CF
		CLIP	BLIP-2	BEiT-3				
<b>Reference-based</b>								
(A)	adaptive	✓				53.7	53.0	35.8
(B)	adaptive	✓	✓	✓	✓	<b>60.4</b>	<b>58.6</b>	<b>38.6</b>
<b>Reference-free</b>								
(C)	adaptive	✓				51.6	51.1	33.8
(D)	adaptive	✓	✓	✓	✓	<b>58.4</b>	<b>56.6</b>	<b>37.8</b>

Table 7: Additional results of feature extractor ablation. We removed all encoders except the CLIP encoder to assess the impact of CLIP. “ $\tau_b$ ” and “ $\tau_c$ ” represents the Kendall’s  $\tau_b$  and  $\tau_c$  correlation coefficient, respectively.

and the inference time was approximately 8.2 ms/sample.

## Appendix D: Additional Experiments

### Additional Comparison with Baselines

Table 5 shows a quantitative comparison with additional baselines, including BERTScore (Zhang et al. 2020), BARTScore (Yuan, Neubig et al. 2021), SPARCS (Feinglass and Yang 2021), and BRIDGE (Sarto, Cornia et al. 2024), which were omitted from the main body due to space constraints. These results demonstrated that Pearl consistently outperformed these baselines on the Composite, Flickr8K-Expert, Flickr8K-CF, and Nebula datasets, demonstrating its superior effectiveness.

### Additional Ablation Studies

**ARSM ablation in reference-free settings.** Table 6 shows the ARSM ablation and the feature extractor ablation in reference-free setting. Metric (i) yielded correlation coefficients of 30.7, 30.4, 16.7, and 42.3 for Composite, Flickr8K-Expert, Flickr8K-CF, and Nebula, respectively. These values decreased by 27.7, 26.2, 21.1, and 10.7 points compared with those of Metric (viii).

Moreover, Metric (iii) yielded correlation coefficients of 58.2, 55.4, 36.7 and 49.3 for Composite, Flickr8K-Expert, Flickr8K-CF, and Nebula, respectively. These values decreased by 0.2, 1.2, 0.9, and 3.7 points compared with those of Metric (viii). These results indicate that ARSM was effective at extracting significant features for automatic evaluation and significantly contributed to performance in reference-free settings.

**Feature extractor ablation in reference-free settings.** We investigated the contribution of image and text encoders by removing CLIP, BLIP-2, BEiT-3, and Stella in the reference-free settings. Table 6 demonstrates the correlation coefficients in the reference-free setting. Using Metric (v) were 55.0, 53.5, 35.5 and 51.5 on Composite, Flickr8K-Expert, Flickr8K-CF, and Nebula, respectively. These values marked decreases of 3.4, 3.1, 2.3 and 1.5 points compared with those of Metric (viii). These results indicate that CLIP significantly contributed to the performance of Pearl in reference-free settings.

As aforementioned in the *Experiments* section, these results do not indicate that CLIP is the sole contributor to

Metrics	Training Dataset	Com	Ex	CF
		$\tau_c$	$\tau_c$	$\tau_b$
<b>Reference-based</b>				
(A)	Nebula	59.2	57.7	37.9
(B)	Ref-based Spica	59.9	56.2	38.3
(C)	Spica	<b>60.4</b>	<b>58.6</b>	<b>38.6</b>
<b>Reference-free</b>				
(D)	Nebula	57.4	51.7	37.1
(E)	Ref-free Spica	57.5	56.2	37.7
(F)	Spica	<b>58.4</b>	<b>56.6</b>	<b>37.8</b>

Table 8: Results of Spica ablation and single-model ablation. “Com”, “EX” and “CF” represent Composite, Flickr8K-Ex and Flickr8K-CF, respectively.

Pearl’s performance. To further investigate this, we conducted an additional ablation study. Table 7 shows the results of the ablation study in which all encoders except the CLIP encoder were removed to assess the impact of CLIP. Compared to the original Pearl (B) and (D), the CLIP-only variants (A) and (C) exhibit a significant performance drop. Results from Tables 6 and 8 indicate that the combination of CLIP, BLIP-2, BEiT-3, and Stella encoders contributed substantially to the overall performance.

**Spica ablation** We evaluated the effectiveness of the Spica dataset by training an existing supervised metric on Spica in both reference-based and reference-free settings. Table 8 presents the results of the Spica ablation. As shown in this table, Pearl trained on Spica (Metrics (C) and (F)) outperformed the model trained on Nebula (Metrics (A) and (D)) in both settings. These results demonstrate the contribution of the Spica dataset to overall performance.

**Single-model ablation.** Pearl adopts a single-model strategy that jointly addresses both settings because this design allows all samples – whether reference-based or reference-free – to contribute to training (See the *Methodology* section.) To evaluate the effectiveness of this strategy, we split Spica into two subsets based on the presence or absence of reference captions and trained Pearl on each subset. Specifically, we created a “Ref-based Spica” subset containing only samples with references, and a “Ref-free Spica” subset containing only samples without references. Table 3

Description	#Error
Descriptiveness Error	42
Relevance Error	40
Annotation Errors	9
Fluency Error	5
Others	4
<b>Total</b>	<b>100</b>

Table 9: Categorization of failure modes. We analyzed the 100 samples with the greatest absolute differences between  $\hat{y}$  and  $y$ .

presents the results of this single-model ablation on Composite, Flickr8K-EX, and Flickr8K-CF. Compared to the original Pearl (C), the variant trained on Ref-based Spica (B) shows a performance drop across all benchmarks, with the largest decrease observed on Flickr8K-Expert (-2.0 points). Similarly, the variant trained on Ref-free Spica (E) also underperformed compared to the original model (F). These results indicate that the single-model strategy contributed to overall performance.

### Appendix E: Error Analysis

The effectiveness of our metric was validated on standard image captioning benchmarks; however, it does come with limitations. To examine these limitations, we analyzed the 100 samples with the greatest absolute differences between  $\hat{y}$  and  $y$ . Table 9 summarizes the failure modes into five primary categories:

- Descriptiveness error: This category includes samples where our metric assigned incorrect scores to captions that lacked descriptiveness.
- Relevance error: This category includes samples where the metric assigned inappropriate scores to candidates with incorrect details.
- Annotation errors: This category includes samples where the human judgments were inappropriate.
- Fluency error: This category includes samples where the metric assigned inappropriate scores to captions containing grammatical errors.
- Others: This category includes miscellaneous errors that do not fall into the above categories.